The Zipper Foldings of the Diamond

Erin W. Chambers* Di Fang Kyle A. Sykes* Cynthia M. Traub†
Philip Trettenero

Abstract

In this paper, we classify and compute the convex foldings of a particular rhombus that are obtained via a zipper folding along the boundary of the shape. In the process, we explore computational aspects of this problem; in particular, we outline several useful techniques for computing both the edge set of the final polyhedron and its three-dimensional coordinates. We partition the set of possible zipper starting points into subintervals representing equivalence classes induced by these edge sets. In addition, we explore non-convex foldings of this shape which are obtained by using a zipper starting point outside of the interval corresponding to a set of edges where the polygon folds to a convex polyhedron; surprisingly, this results in multiple families of non-convex and easily computable polyhedra.

1 Introduction

A folding of a polygon is a gluing of the points on the perimeter together to form a polyhedron. A theorem of Alexandrov shows that as long as sum of angles at every glued point is no more than 2π, then every folding of a convex polygon leads to unique convex polyhedron (in which a doubly covered polygon is considered a "flat" polyhedron) [4]. If a folding meets the requirements for Alexandrov's theorem then we are given the existence of a convex polyhedron corresponding to the folding. A more recent constructive proof by Bobenko and Izmestiev allows for the explicit construction of a polyhedron by solving a certain differential equation [6]. An implementation of the constructive algorithm has been coded by Stefan Sechelmann[1]. Given any input triangulation of the polygon with gluing instructions, the implementation will output the final polyhedron. However, this particular implementation does not return the corresponding triangulation on the polygon. The algorithm runs in pseudopolynomial time since the algorithm must take the initial triangulation and flip it to a geodesic triangulation, which is not in general a polynomial time operation [11].

We seek a more combinatorial approach to computing this information. Given a set of gluing rules corresponding to a zipper folding, we outline an approach for computing the crease patterns (i.e., characterize and predict the combinatorial structure of edges and faces) as well as the exact location of the vertices.

Related work. Work has been done towards determining all the combinatorially different convex polyhedra obtained via foldings, primarily for regular convex polygons as well as a few other shapes such as the Latin cross [12, 5, 1, 2, 3]. In each work, the authors must determine the set of line segments in the polygon which become edges in the final polyhedron; we refer to these edges as the *crease pattern* for the shape. Note that the crease pattern may not contain all boundary edges of the original polygon; see Figure 8 for an example of when the polyhedral edges "cross" the boundary of the original polygon.

In [5] (and later in [7]), all (combinatorially distinct) convex polyhedra foldable from a square are determined using a combinatorial structure called gluing trees. Crease patterns and reconstructions of the folded polyhedra are also given, making the study of foldings of the square complete. In [1, 2, 3], the focus is on determining all foldings of regular n-gons, without focusing on reconstructing the actual polyhedron.

*Department of Mathematics and Computer Science, Saint Louis University, {echambe5,ksykes2}@slu.edu.
†Department of Mathematics and Statistics, Southern Illinois University at Edwardsville, cytraub@siue.edu
[1] http://www3.math.tu-berlin.de/geometrie/ps/software.shtml\#AlexandrovPolyhedron

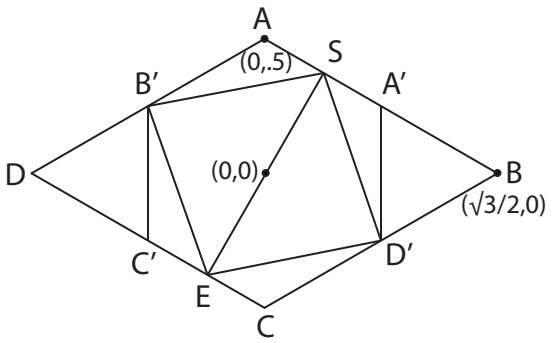

Figure 1: The crease pattern at $\epsilon = 1/4$, which has a 3-regular adjacency graph.

There is also related work which examines when the Platonic solids can be "unzipped" to a polygonal net and rezipped into a doubly covered flat polygon [13]; a different paper considers finding different tetrahedra which "unzip" to a common polygonal net [14]. A complete analysis of polyhedra zipper foldable from the 1×2 rectangle is given in [15], utilizing the techniques outlined here.

As previously mentioned, our primary goal here was to seek a simpler combinatorial approach to verify correct crease patterns in a restricted type of folding. To that end, we consider a restricted class of foldings using the perimeter-halving method, where the perimeter of the polygon is identified starting from a specified point gluing together points equidistant from the starting point (as measured along the perimeter), which "zips" up the boundary of the polygon into a polyhedron. We will use the term *zipper foldings*, which was first introduced in Demaine et al [10]); a related special case is the class of pita polyhedra which arise from zipper folding regular polygons [7]. As far as the actual resulting polyhedra, surprisingly little is known even about this simple class of foldings aside from the previously mentioned papers which (like ours) consider a particular shape and examine it in detail [1, 2, 3, 5].

Predicting creases. As was observed by Alexandrov and noted in [5], there are a finite number of possible crease patterns. However, in our experience, verifying or discounting a crease pattern has been surprisingly difficult in more complex polygons, since checking a crease pattern either involves seeing if a paper model will fold (highly prone to error) or attempting to compute the folding in a program such as Mathematica (which can lead to numerical issues). As a result, most prior combinatorial work on computing zipper foldings was done using ad hoc methods.

We describe now points on the polygon which will be of interest as we construct the corresponding polyhedron via zipper folding. Our initial polygon is the equilateral rhombus (or diamond) centered on the origin with unit edge length and interior angles $60°$ and $120°$. Label the vertices A, B, C, D; see Figure 1 for an example of the labeling. Let the starting point of our zipping S be a point on edge AB located at $(\frac{\sqrt{3}\epsilon}{2}, \frac{1-\epsilon}{2})$, and refer to the location of S by this ϵ. Note that $0 \leq \epsilon \leq 1$, and the location of S is distance ϵ from point A along edge AB. The point E on edge CD is the reflection of S through the origin, which is where the zipper "ends". For any such folding, we will use A', B', C', D' to denote the points on the boundary of the polygon which glue to A, B, C, D, respectively.

As previously mentioned, for polygonal foldings in general, it is known that if the requirements for Alexandrov's theorem are satisfied then there exists a valid folding. Here, we present several computational reconstruction techniques which may be of interest in this area. We also develop several methods to prove that a particular crease pattern is valid as the start point moves along a continuous interval on the boundary; previous papers seem to have relied on numerical approximation to verify validity, which will reach its limit as the polygon becomes more complex. We also classify all the zipper foldings resulting from the diamond outlined above.

Theorem 1. *There are 21 combinatorially distinct convex polyhedra resulting from zipper foldings of a diamond. There are 7 polyhedra which have non-triangular faces and 4 "flat" polyhedra, all of which occur at isolated points where the crease pattern changes.*

The polyhedra shown in Figure 1 represent the 10 polyhedra with triangular faces, and the solid dots represent the 11 isolated polyhedra noted above. The polyhedra with triangular faces form octahedra. Together, these represent all the zipper foldings of the diamond.

2 Computing the foldings

In our foldings, all polyhedra will have at most 6 vertices, resulting from gluing each of A, B, C, and D to some other point on the perimeter, as well as the vertices S and E. We are often interested in the actual adjacencies in the final folded polyhedron; this network of edges forms an adjacency graph, often called the graph of the polyhedron, on the (at most) 6 vertices. We refer to this adjacency graph as the *crease pattern*.

Our techniques for computing these foldings break down into several relevant categories. The first (and simplest) are the flat foldings when the entire polygon folds into a doubly-covered polygon. For example, when $\epsilon = 0$, the vertices B and D zip together and the result is a flat doubly covered regular triangle; flat foldings also occur when $\epsilon = .5, .75$, and 1.

The remaining cases in our computation are handled based on whether the graph of the polyhedron is 4-regular or not; if not, in our shape, as well as in the 1×2 rectangle studied in [15], the graph will always consist of vertices of degrees 3, 4, and 5. When degree-3 vertices exist, as discussed in Section 2.1, computing the crease pattern is much simpler, since it is not difficult to verify that the underlying structure of the polyhedron can be decomposed into several tetrahedra. The more complex 4-regular case requires additional techniques to calculate exactly; we detail these techniques in Section 2.2. In addition, further complexity arises when the boundary edges of the initial polygon do not become edges in the final polyhedron; see for example the crease patterns in Figure 1 which are nearest to $\epsilon = 1$. These patterns, which occur much more often in this shape than previous related work, required an extra set of tools to calculate correct crease patterns and 3-D realizations. In Section 2.3, we examine these tools which require zipper folding a related *non-convex* polygon to yield the same polyhedron.

In Figure 3, we show the creases with marked points for the places where the crease pattern undergoes a combinatorial change, which we call a *transition*. Note that (as in previous work) at most of these transitions, two triangles become co-planar to form a quadrilateral (indicated as a dotted line) and then the opposite quadrilateral diagonal appears in the polyhedron. All other transitions occur when the polyhedron folds to a flat doubly covered polygon.

2.1 Degree-3 vertices in the pattern

Crease patterns with at least one degree-3 vertex are substantially easier to realize in $\mathbb{R}^3$, computationally speaking. In this shape, this results from the fact when we have such a graph with our setup, we can decompose the final polyhedron into three tetrahedra (two "outer" tetrahedra and the "inner" tetrahedron). In Figure 4, we show the adjacency graph of the polyhedron generated when $\epsilon = 1/4$. Figure 5 shows the reconstruction of the two outer tetrahedra, and Figure 6 shows the final polyhedron decomposed into three tetrahedra, where the inner tetrahedron is composed of two triangles from the outer tetrahedra which meet on an edge, plus a single additional edge.

For values of ϵ in intervals with a degree-3 vertex in the crease pattern, we wrote code to find exact coordinates for the three-dimensional polyhedron that results. Reconstructing a tetrahedron using adjacencies and edge lengths is not difficult to do, so the general approach we used was to reconstruct the inside tetrahedron shown in Figure 6, and then reconstruct the outer tetrahedra. We next illustrate this process via an example.

Consider the crease pattern at $\epsilon = 1/4$. This crease pattern contains the edges SE and BD. In its initial configuration, we note that points B and D are both adjacent to SE as well as to each other. We can leave

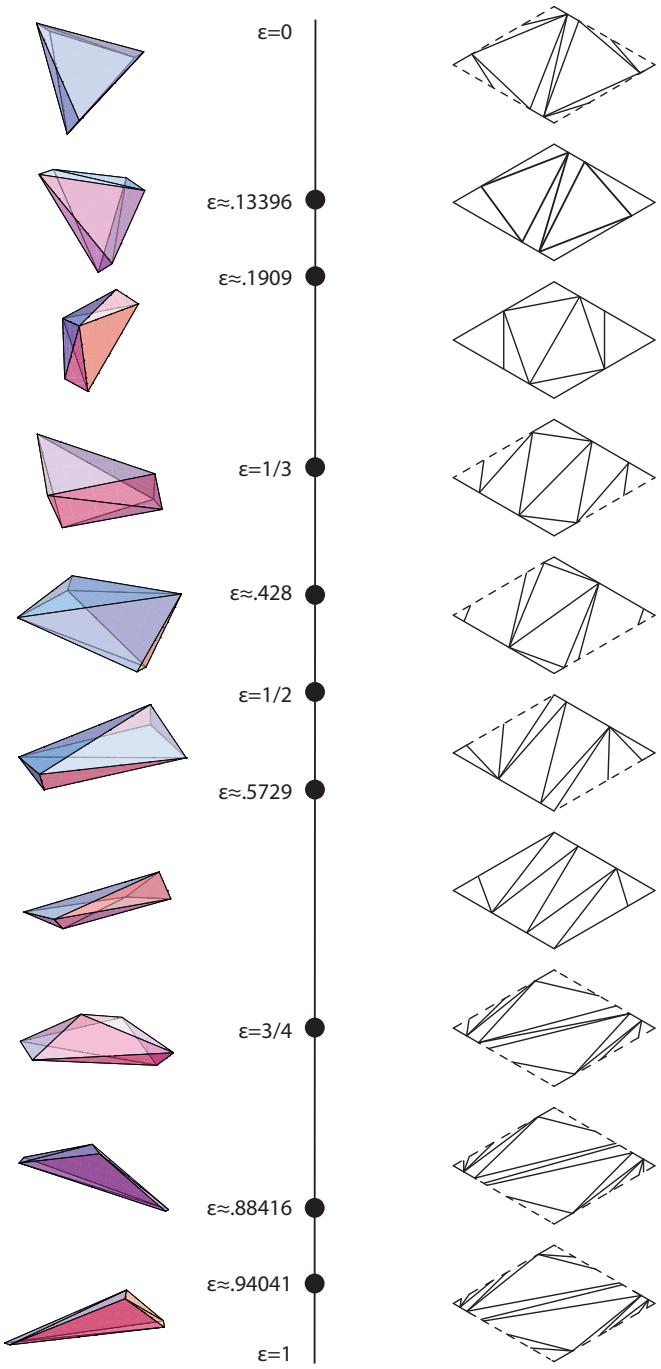

Figure 2: All the crease patterns for the zipper foldings of the diamond as the start point S varies by distance ϵ from point A along edge AB. Images are taken from sample values between each transition point, marked with solid dots. Dashed lines indicate that a crease extends over an edge. The polyhedra shown between transition points correspond with the respective crease patterns. The symmetry of our input shape allows us to study all zipper foldings by varying the location of S along one edge; moving S to another edge will give a combinatorially equivalent folding.

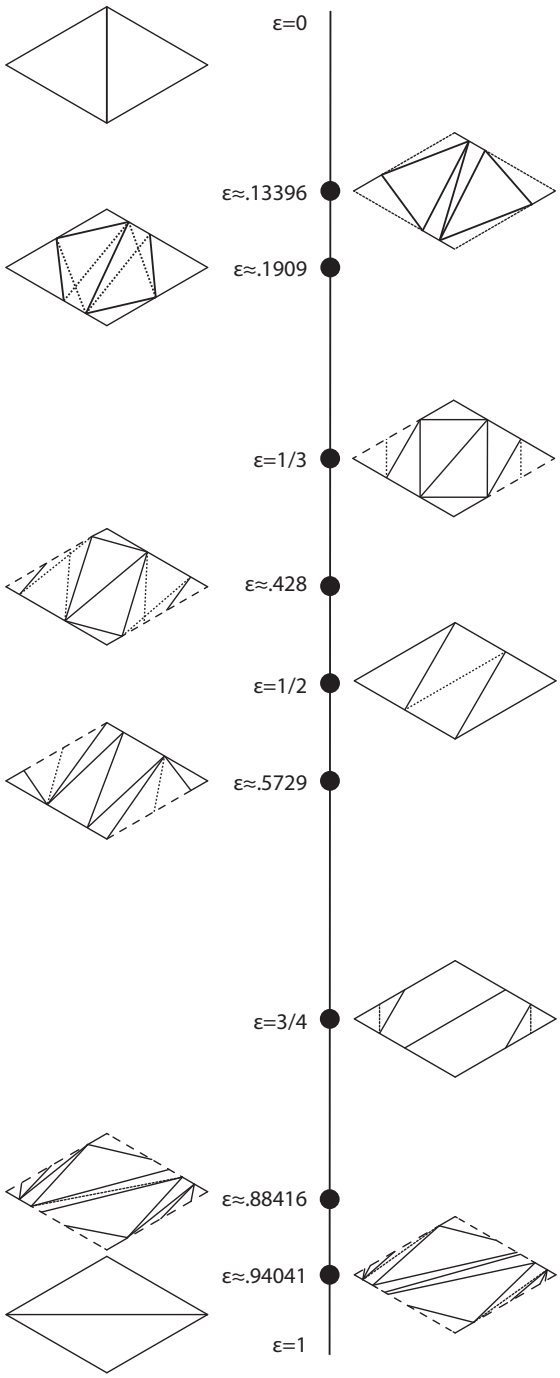

Figure 3: All the crease patterns at each transition point (which are marked by black dots). Dashed lines indicate that a crease extends over an edge. Dotted lines indicate interior diagonals of a quadrilateral face that are realized as polyhedral edges on either side of the transition point.

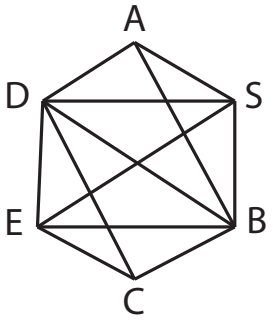

Figure 4: The graph of the polyhedron for $\epsilon = 1/4$

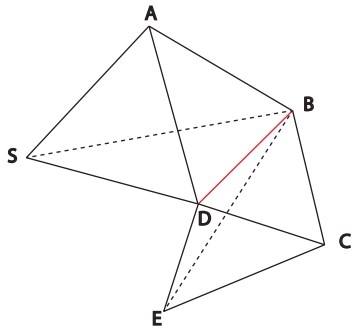

Figure 5: The two "outer" tetrahedra of the polyhedron joined along the common edge $\overline{BD}$.

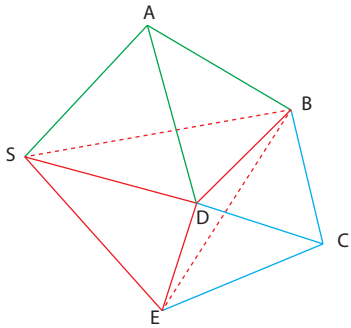

Figure 6: The final polyhedron decomposed into three tetrahedra.

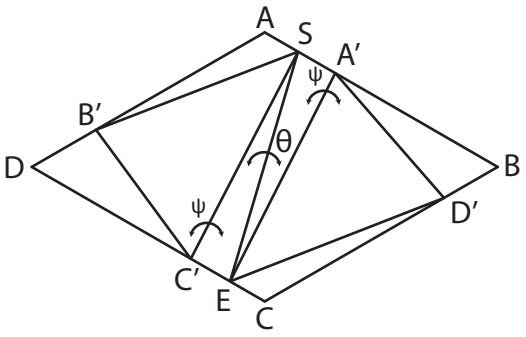

Figure 7: A crease pattern whose adjacency graph is 4-regular to illustrate the reconstruction process.

edge SE fixed in the $z = 0$ plane. Rotate points B' and D' by θ about edge SE into the positive z-direction. We solve for the value of θ which positions points B' and D' at the correct final distance $|B'D| = 2\epsilon$ from each other; this establishes a central "tetrahedron" within our final polygon. Vertex A is adjacent to B', D', S, and hence can be located by solving a system of 3 distance equations. Similarly, C is adjacent to B', D', E. The resulting figure is convex and has edge lengths that match those from the polygonal net.

To extend from a specific value of ϵ to the entire interval containing ϵ, we note that the ability to construct the "central" tetrahedron $BDSE$ for S corresponding to a specific $0.1909 < \epsilon < 1/3$ can be verified via an intermediate value theorem argument. Simply measure the distance between B and D when the dihedral angle at SE is 0 and again when it is π. If the desired length of BD is between these two values, then folding over SE by some angle $0 \leq \theta \leq \pi$ will attain the correct length for BD. Then, checking the angle criterion given in Lemma 2 (see appendix) confirms that locations for points A and C can be found that realize all desired distances. It remains only to verify that the resulting polyhedron is convex. Since for ϵ values in this interval, the orthogonal projection of A onto the plane containing triangle BDS is interior to triangle BDS, the final polyhedron will be convex.

2.2 4-regular graph of the polyhedron

In folding patterns where all vertices are degree-4, realization of the vertices in $\mathbb{R}^3$ is not as simple as degree-3 case. In [7], the authors describe a method for constructing an octahedron by splitting it into 2 smaller hexahedra which share an edge that is an internal diagonal of the octahedron. They vary the length of this edge until the dihedral angles of the faces incident to the edge match. We utilize a different method that also reduces a partial polyhedron to one parameter of change. We illustrate this for ϵ in the interval $.13396 < \epsilon < .1909$; the crease pattern for this range is shown in Figure 7.

We consider the following flex over edge SE. Fold triangles SEA' and SEC' upward from the $z = 0$ plane each by angle θ, leaving edge SE fixed in the plane. Each choice of θ results in a fixed measure of $\angle A'SC'$ and $\angle A'EC'$. The two remaining triangular faces $SB'C'$ and ASB' which are incident to S (or respectively E) are uniquely configurable into a shell comprised of faces of the final convex polyhedron. That is, of the two locations in $\mathbb{R}^3$ for point B_θ that give correct distances for segments AB, BC, BS, only one is extendable into a convex polyhedron. We similarly find a location for D_θ. (The subscripts here serve as a reminder that the locations of B_θ and D_θ depend on the initial flex by angle θ.) Note that this convex shell contains six of the eight faces of the final polyhedron; the two missing faces must share a common edge. We then vary θ to realize the correct length for this missing common edge; if no such θ exists, then we can reject this crease pattern. Moreover, we can also reject the pattern if the final folding results in a non-convex polyhedron; else, it must realize a convex folding of the initial crease pattern.

2.3 Creases over the boundary of the polygon

While the particular approach varies slightly, this process from the previous section can be repeated for any 4-regular graph of the polyhedron. However, some complications arise when the crease pattern is more complex. For example, consider the crease pattern when the source of the zipper S is near B. In this case, many of the edges in the final polyhedron actually cross an edge of the initial polygon, since not all of the polygon's edges are edges of the final polyhedron. (This also occurs at several other positions; see Figure 1.) Computationally speaking, these patterns are more difficult because a single crease is split into different segments inside the polygon. In order to compute these foldings, we altered the original polygon to be *non-convex* and verified the crease pattern in this related polygon.

One example occurs when the zipper point reaches near point B in our shape, for the crease patterns above $\epsilon = .75$; see Figure 8 for the pattern at $\epsilon = 7/8$. Here, the creases cross over the edges AB' (and by symmetry also BA') as well as $C'D$ (and DC'). Using the original gluing information, we reconstructed an equivalent non-convex polygon which folded to an identical polyhedron and allowed for easier computation, given the symmetry and reduction in the number of creases.

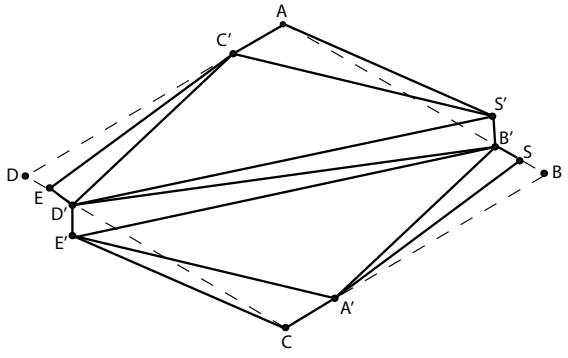

Figure 8: The crease pattern for $\epsilon = 7/8$ rearranged to a non-convex polygon.

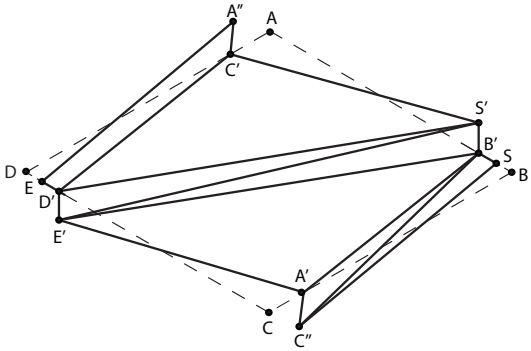

Figure 9: The crease pattern for the range just below 1 rearranged to a non-convex polygon.

This set of crossings becomes even more drastic as the zipper point nears B, which is a vertex of high curvature. The crossing edges do not change, but the rearranged figure becomes more complex due to extra crossings, and the non-convex polygon in turn becomes more complex. See Figure 9 for the final rearranged figure just below $\epsilon = 1$.

A very different example occurs for the crease pattern at $\epsilon = 1/10$; here, instead of keeping the shape close to the original diamond, we more drastically rearrange to take advantage of symmetry when computing the folding. This crease pattern contains the edges SE and BD. However, in its initial configuration, we note that points A' and C' are both adjacent to SE, but A and C are not adjacent to each other in the final polyhedron. We use the gluing instructions to rearrange the triangular faces so that they are as in Figure 10. Now vertices S and E are both incident to edge BD so we can fold this polygon symmetrically, leaving edge BD fixed in the $z = 0$ plane and proceed exactly as outlined in the $\epsilon = 1/4$ case described in Section 2.1.

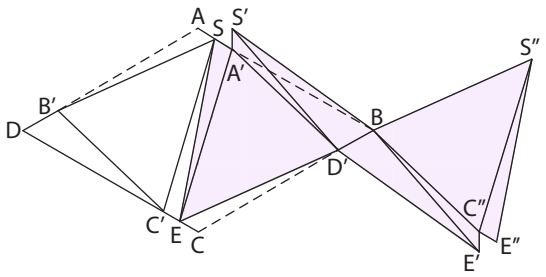

Figure 10: A crease pattern for a convex polyhedron when $\epsilon = 1/10$. The initial net is diamond $ABCD$. The shaded faces are shown rearranged to match the algorithmic approach to reconstruction.

For nets where the vertices incident to the crease through $(0, 0)$ are adjacent, this rearranging of the net is not always needed. We do take advantage of this rearrangement technique whenever a three-dimensional edge of our final polyhedron intersects a two-dimensional boundary edge of our initial polygon. Since the gluing instructions are preserved, this is merely a bookkeeping tool that allows for easier computations.

3 Non-convex polyhedra

One interesting result of our investigation of this pattern is a natural classification of some types of *non-convex* foldings, which to the best of our knowledge have not been a focus of investigation in related work on zipper foldings. It is known of course that convex shapes will fold to non-convex polyhedra, and work has been done on counting the number of foldings of a shape; see for example [9]. In addition, recent work has focused on unfolding a polyhedron to a convex shape and then refolding it to a different (convex) polyhedron [8]; in contrast, our results consider zipper folding a convex planar shape to one or more non-convex polyhedra, which seems an interesting variant of refold rigidity.

The main point of interest is how easy these non-convex foldings are to find computationally speaking. These foldings result from pushing a particular crease pattern past the point where two faces become coplanar and a "flip" in the crease pattern occurs. In our experiments, the primary method to establish the validity of a crease pattern is by finding a solution in $\mathbb{R}^3$ to a system of quadratic equations defining pairwise distances, then checking the convexity of the resulting polyhedron. These non-convex foldings appeared when the code for computing a solution ran successfully but failed the convexity check.

For an example of these, consider Figure 11. In the example shown on the left, we consider when the zipper point is at $\epsilon = .36$. However, instead of using the correct crease pattern shown in Figure 1, we are instead using the crease pattern for the interval below $\epsilon = 1/3$. Similarly, on the right side of Figure 11, we have a non-convex folding when $\epsilon = 1/6$, but the crease pattern used is the one that is valid for the interval above $\epsilon \approx .1909$. In this second picture, we have actually pushed the non-convex folding as far is it will

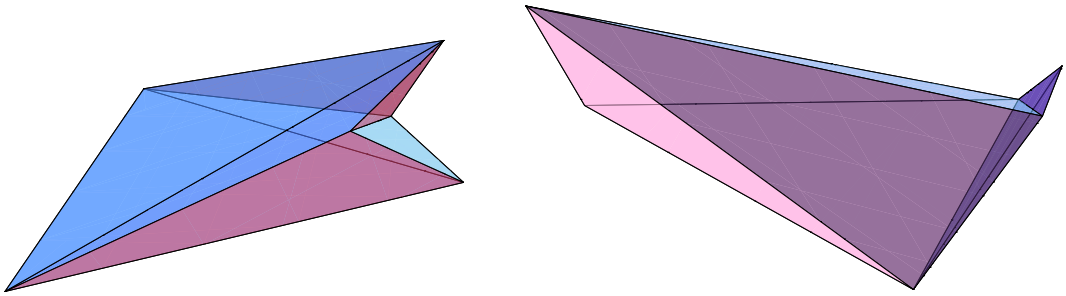

Figure 11: Top: a non-convex folding when the zipper source is at $\epsilon = .36$. Bottom: A non-convex folding when $\epsilon = 1/6$; here, the folding results in a flat flap, indicating that this crease pattern will not fold to a polyhedron at all when pushed lower than 1/6.

extend, since using this crease pattern for any lower value of ϵ will result in an invalid folding (where the polygon self-intersects).

These calculations lead us to conjecture that any valid crease pattern over an interval will fold to a non-convex polyhedron for some value of ϵ close to the interval of convexity. This conjecture is certainly true in our shape (except near flat foldings), and it seems likely to hold for other shapes since convexity does not impact the existence of a solution.

4 Future directions

We have focused here on zipper foldings of this particular shape. In much of the previous work in this area, all the foldings of a convex shape have been determined using techniques such as gluing trees. Using those techniques to calculate all the convex foldings of this diamond remains an area to address.

Another interesting question is to determine the relationship between the zipper foldings we discuss here with the zipper foldings of the square, as they appear similar [5, 7]. A link between the diamond and square zipper foldings might give a list of constraints for when two "similar" figures have "similar" foldings. Similar lines of questioning could be asked about rhombi in general. For instance, if the edge lengths are similarly defined, are the values of ϵ where transitions occur similar?

The non-convex foldings described in Section 3 are also perhaps worth further investigation in other shapes. It would also be interesting to examine when these non-convex foldings cease to be valid, and to try to discover how many valid (non-convex) crease patterns might be present at a particular zipper point.

Acknowledgements

This research was supported in part by the National Science Foundation under Grant No. CCF 1054779, as well as an REU supplemental to that grant.

References

[1] J. Akiyama and G. Nakamura. Foldings of regular polygons to convex polyhedra ii: Regular pentagons. *J. Indones. Math. Soc.(MIHMI) Vol*, 9:89–99, 2003.

[2] J. Akiyama and G. Nakamura. Foldings of regular polygons to convex polyhedra iii: Regular hexagons and regular n-gons, n 7. *Thai Journal of Mathematics*, 2(1):1–15, 2004.

[3] J. Akiyama and G. Nakamura. Foldings of regular polygons to convex polyhedra i: Equilateral triangles. *Combinatorial Geometry and Graph Theory*, pages 34–43, 2005.

[4] A.D Aleksandrov. Konvexe polyeder. *Akademie Verlag*, 1958.

[5] Rebecca Alexander, Heather Dyson, and Joseph O'Rourke. The foldings of a square to convex polyhedra. In Jin Akiyama and Mikio Kano, editors, *Japanese Conference on Discrete and Computational Geometry*, volume 2866 of *Lecture Notes in Computer Science*, pages 38–50. Springer Berlin Heidelberg, 2003.

[6] A.I. Bobenko and I. Izmestiev. Alexandrov's theorem, weighted delaunay triangulations, and mixed volumes. In *Annales de l'institut Fourier*, volume 58, pages 447–506. Chartres: L'Institut, 1950-, 2008.

[7] E.D. Demaine and J. O'Rourke. *Geometric folding algorithms: linkages, origami, polyhedra*. Cambridge University Press, 2008.

[8] Erik D. Demaine, Martin L. Demaine, Jin ichi Itoh, Anna Lubiw, Chie Nara, and Joseph O'Rourke. Refold rigidity of convex polyhedra. In Abstracts from the 28th European Workshop on Computational Geometry, 2012.

[9] Erik D. Demaine, Martin L. Demaine, Anna Lubiw, and Joseph O'Rourke. Examples, counterexamples, and enumeration results for foldings and unfoldings between polygons and polytopes. Technical Report 069, Smith, 2000.

[10] Erik D. Demaine, Martin L. Demaine, Anna Lubiw, Arlo Shallit, and Jonah L. Shallit. Zipper unfoldings of polyhedral complexes. In *Proceedings of the 22nd Canadian Conference on Computational Geometry*, pages 219–222, 2010.

[11] Daniel Kane, Gregory N. Price, and Erik D. Demaine. A pseudopolynomial algorithm for alexandrov's theorem. In *Proceedings of the 11th International Symposium on Algorithms and Data Structures*, WADS '09, pages 435–446, Berlin, Heidelberg, 2009. Springer-Verlag.

[12] A. Lubiw and J. O'Rourke. When can a polygon fold to a polytope. In *AMS Conference*, 1996.

[13] Joseph O'Rourke. Flat zipper-unfolding pairs for platonic solids. *CoRR*, abs/1010.2450, 2010.

[14] Joseph O'Rourke. Common edge-unzippings for tetrahedra. *CoRR*, abs/1105.5401, 2011.

[15] Katherine Schwent. Perimeter-halving the one-by-two rectangle. Master's thesis, Southern Illinois University Edwardsville, 2013.

A Realizing tetrahedra

In our discussion of calculating the folding where there is a degree-3 vertex in the graph of the polyhedron, we need a characterization of when a set of vertices and edges can be realized in $\mathbb{R}^3$ as a tetrahedron. We then use this to help us discover the entire range along which the tetrahedron is present in the final folding. We summarize this tool in the following lemma:

Lemma 2. *A net of four triangles as shown in Figure 12 will fold to a tetrahedron if*

1. *Lengths of corresponding sides are equal. ($|AF| = |EF|, |AB| = |BC|$, and $|CD| = |DE|$)*
2. *At each vertex, the angle of the base is less than the sum of the other two incident face angles.*

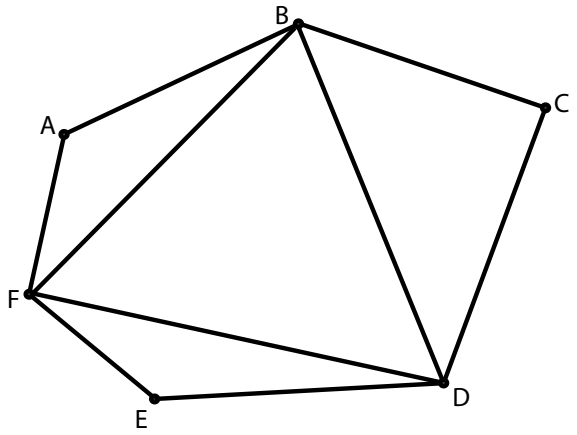

Figure 12: Corresponding figure for Lemma 2

Proof. It is clear that the first condition is necessary, since within the tetrahedron, points A, C, E will all be identified and thus corresponding edge lengths must be the same. To verify the second condition, we show that, without loss of generality, all points incident to F can be realized in three dimensions. Assume $\angle BFD \leq \angle AFB + \angle DFE$. If this condition were not met, then no position of point A rotated over segment BF will coincide with any position of point E rotated over DF. When the angle criterion is satisfied, let X be a point in $\mathbb{R}^3$ where points A and E coincide after rotations over BF and DF respectively. We know by condition 1 that $|XB| = |AB| = |CB|$ and $|XD| = |ED| = |CD|$, so triangle $\triangle BCD$ will fold into position over edge BD with C identified with point X to complete the tetrahedron. □